Glutamatergic postsynaptic density in early life stress programming: Topographic gene expression of mGlu5 receptors and Homer proteins

Elisabetta F. Buonaguro, Sara Morley-Fletcher, Camilla Avagliano, Licia Vellucci, Felice Iasevoli, Hammou Bouwalerh, Gilles van Camp, Ferdinando Nicoletti, Stefania Maccari, Andrea de Bartolomeis

Glutamatergic postsynaptic density in early life stress programming: Topographic gene expression of mGlu5 receptors and Homer proteins

[&]Elisabetta Filomena Buonaguro[1], [&]Sara Morley-Fletcher[2,6], Camilla Avagliano[1], Licia Vellucci[1], Felice Iasevoli[1], Hammou Bouwalerh[2,6], Gilles Van Camp[2,6], [#]Ferdinando Nicoletti[3,4], *[#]Stefania Maccari[2,5], Andrea de Bartolomeis[1]

[1]Laboratory of Molecular and Translational Psychiatry, Unit of Treatment Resistant Psychosis, Section of Psychiatry and Psychology, Department of Neuroscience, Reproductive Science and Odontostomatology University of Naples Federico II, Naples, Italy

[2]Universiy of Lille, CNRS, UMR 8576 - UGSF - Unité de Glycobiologie Structurale et Fonctionnelle, F-59000 Lille, France

[3]IRCCS Neuromed, 86077, Italy

[4]Department of Human Physiology and Pharmacology Sapienza University of Rome, Rome, Italy

[5]Department of Medico-Surgical Sciences and Biotechnology, Sapienza University of Rome, Rome, Italy

[6]International Associated Laboratory (LIA), France/Italy "Prenatal Stress and Neurodegenerative Diseases." University of Lille – CNRS, UMR 8576 and Sapienza University of Rome - IRCCS Neuromed

#Co-director of LIA France/Italy

[&]These authors contributed equally

Correspondence to: * Prof. Stefania Maccari, 2PhDs,

Co-director of LIA, Head of "Glycobiology of Stress-related Disorders" Team in UMR 8576, UGSF, 59665 Villeneuve d'Ascq, France

Abstract

Type-5 metabotropic glutamate receptors (mGlu5) have been implicated in the mechanism of resilience to stress. They form part of the postsynaptic density (PSD), a thickening of the glutamatergic synapse that acts as a multimodal hub for multiple cellular signaling. Perinatal stress in rats triggers alterations that make adult offspring less resilient to stress. In the present study, we examined the expression of gene encoding the mGlu5 (*Grm5*), as well as those encoding the short and long isoforms of Homer proteins in different brain regions of the offspring of dams exposed to repeated episodes of restraint stress during pregnancy ("perinatally stressed" or PRS offspring). To this end, we investigated unconditioned behavioral response using the light/dark box test, as well as the expression of PSD genes (*Homer1a*, *Homer1b*, and *Grm5*), in the medial prefrontal cortex, cortex, caudate-putamen, amygdala, and dorsal hippocampus. PRS rats spent significantly less time in the light area than the control group. In the amygdala, *Homer1a* mRNA levels were significantly increased in PRS rats, whereas *Homer1b* and *Grm5* mRNA levels were reduced. In contrast, the transcript encoding for *Homer1a* was significantly reduced in the medial prefrontal cortex, caudate-putamen, and dorsal hippocampus of PRS rats. We also evaluated the relative ratio between *Homer1a* and *Homer1b/Grm5* expression, finding a significant shift toward the expression of *Homer1a* in the amygdala and towards *Homer1b/Grm5* in the other brain regions. These topographic patterns of *Homer1a*, *Homer1b,* and *mGlu5* gene expression were significantly correlated with risk-taking behavior measured in the light/dark box test. Remarkably, in the amygdala and in other brain regions, *Homer1b* and *Grm5* expression showed positive correlation with time spent in the light box, whereas *Homer1a* in the amygdala showed a negative correlation with risk-taking behavior, in contrast with all other brain regions analyzed, wherein these correlations were positive. These results suggest that perinatal stress programs the developmental expression of PSD molecules involved in mGlu5 signaling in discrete brain regions, with a predominant role for the amygdala.

Key words: Synapse; Stress; Early life programming; Animal model; Gene expression

Abbreviations

ACC: anterior cingulate cortex

AI: agranular insular cortex

Amy: amygdala

BLA: basolateral amygdala

Cab: core of the nucleus accumbens

CP: Caudate Putamen

DG: dentate gyrus

dHPC: dorsal hippocampus

DL: dorsolateral putamen

DM: dorsomedial putamen

IC: insular cortex

LO: lateral orbital cortex

M2: secondary motor cortex

MeA: medial amygdala

MAC: medial agranular cortex (premotor cortex)

MC: motor cortex

MO: medial orbital cortex

mGluR: type I metabotropic glutamate receptor

mPFC: medial prefrontal cortex

NMDA-R: N-Methyl-D-Aspartate receptor

Prl: prelimbic cortex

Sab: shell of the nucleus accumbens

SS: somatosensory cortex

VL: ventrolateral putamen

VM: ventromedial putamen

VO: ventral orbital cortex

1. Introduction

Stress-related disorders are a major public health issue (Alonso et al., 2007, Lepine 2002). Stress causes profound changes in excitatory and inhibitory synaptic transmission; these have been investigated in various animal models (de Bartolomeis et al., 2017) but only rarely in humans (Shcheglovitov et al., 2013). However, animal studies oversimplify pathologies that are uniquely human, such as psychiatric disorders.

Proteins of the postsynaptic density (PSD) play a major role in the synaptic response to stress. PSD is a thickening of the glutamatergic synapse that comprises a complex of receptors, scaffolding, and adaptor proteins; it acts as a multimodal hub for multiple cellular signaling (Lum et al., 2016, Soler et al., 2018). The PSD protein network fine-tunes signal transduction, integrating synaptic signals from presynaptic neurons and different neurotransmitter systems (Collins et al., 2006, de Bartolomeis et al., 2005, Gold 2012, Sheng and Hoogenraad 2007). N-Methyl-D-Aspartate (NMDA) receptors, type-I metabotropic glutamate receptors (mGlu1 and mGlu5), and their interacting proteins (Homers) are integral components of the PSD. They have been implicated in stress-induced alterations (Palmfeldt et al., 2016). The induction of *Homer1a*, an immediate early-gene member of the Homer1 family that is involved in glutamate-mediated synaptic plasticity, is part of the mechanism of action of several antidepressant and antipsychotic treatments (Buonaguro et al., 2017a, Buonaguro et al., 2017b, de Bartolomeis et al., 2016, de Bartolomeis et al., 2013, Iasevoli et al., 2014, Serchov et al., 2016). The constitutively expressed splice variants of Homer proteins (e.g., Homer1b and Homer1c) link mGlu5 to the intracellular signaling machinery and mediate the ligand-dependent activity of mGlu5 (Brakeman et al., 1997). Homer1b and other long isoforms of Homer link mGlu5 to NMDA receptors and various signaling molecules, such as inositol-1,4,5-trisphosphate receptors and transient receptor potential ion channels (Bertaso et al., 2010; de Bartolomeis and Tomasetti 2012, Tu et al., 1998, Yuan et al., 2003). In contrast, the short Homer isoform, Homer1a, which is produced by an immediate early gene, acts as a negative dominant signaling molecule, disrupting mGlu5/Homer1b coupling and modulating ligand-independent mGlu5 signaling (Ango et al., 2001). Therefore, Homer1 moderates the NMDA/mGlu5 complex (Bertaso et al., 2010, Tu et al., 1999), which is involved in the activity of the glutamate synapse.

A growing body of evidence suggests that abnormalities of glutamatergic transmission are involved in the regulation of emotions and stress response (Chen et al., 2010, Luoni et al., 2014, Musazzi et al., 2013, Popoli et al., 2011, Vyas et al., 2002). Acute stress-induced release of glucocorticoids enhances extracellular glutamate levels in the hippocampus and prefrontal cortex (Bagley and Moghaddam 1997, Yuen et al., 2009), thereby influencing some aspects of cognitive processing in

rodents (Danysz et al., 1995, Robbins and Murphy 2006). The effects of chronic stress on glutamate release are still mostly unknown, although the few available studies have suggested that chronic stress can reduce glutamate release (Moghaddam 2002, Popoli et al., 2011).

Furthermore, abnormalities of the glutamatergic system may persist in adult animals exposed to stressful manipulation during the perinatal period (Jia et al., 2015, Sun et al., 2013, Zhang et al., 2013), suggesting that adult vulnerability to stress-related diseases may be programmed during perinatal life (Barker et al., 2006, Maccari et al., 2014). The rat model of perinatal stress (PRS) has been widely used to investigate stress-related alterations. Recently, we showed profound and persistent impairment of glutamatergic neurotransmission in PRS rats (Laloux et al., 2012, Marrocco et al., 2012, Marrocco et al., 2014, Zuena et al., 2008), characterized by impaired synaptic activity and reduced depolarization-evoked glutamate release in the ventral hippocampus. Defective glutamate transmission has been causally related to reduced risk-taking behavior (Morley-Fletcher et al., 2018), and it is associated with severe reduction in synaptic vesicle-associated proteins (Marrocco et al., 2012). This deficit at the presynaptic level can be corrected by long-term treatment with antidepressants or carbetocin agonists (Mairesse et al., 2015, Marrocco et al., 2014, Morley-Fletcher et al., 2018). However, to date, no investigations have focused on how PRS can shape synapse architecture at the postsynaptic level or in different brain regions.

Therefore, the present study aimed to investigate the long-term molecular characteristics of PRS rats, focusing on the expression of genes linked to glutamatergic signaling and synaptic plasticity at the level of the PSD, such as *Homer1a*, *Homer1b,* and *Grm5.* We performed a topographic study to explore expression of the above-mentioned transcripts, using *in situ* hybridization in different brain regions related to the stress response to obtain quantitative and qualitative data on gene expression. Finally, we evaluated the relationship between risk-taking behavior and transcript expression within discrete brain subdivisions.

2. Materials and Methods

2.1. Animals

Nulliparous female Sprague-Dawley rats weighing approximately 250 g were housed in the presence of a sexually experienced male rat. A sperm-positive vaginal smear was used to determine embryonic day 0 (E0). Pregnant females were then individually housed under controlled temperature (22°) and humidity (60%) conditions, with *ad libitum* access to food and water. They were kept under a regular 12-hour light/dark cycle (on at 07:00, off at 19:00). At E11, pregnant rats were randomly assigned to gestational stress and control groups. All animal experiments were carried out in accordance with EU Directive 2010/63/EU for animal experiments.

2.2. Gestational stress procedure (perinatal stress in offspring)

Restraint stress was induced according to a previously described protocol (Maccari et al., 1995, Morley-Fletcher et al., 2003). The local ethical committee CEEA-75 (Comité d'Ethique en Expérimentation Animale Nord-Pas de Calais, 75) approved the gestational restraint procedure. Female pregnant rats at E11 were subjected to three 45-minute stress sessions daily until delivery. The sessions started at 09.00, 12.00, and 17.00. Specifically, they were placed in transparent plastic cylinders and exposed to bright light. Control dams were left undisturbed in their home cages.
In both groups, the litters used contained between 8 and 14 pups. Offspring were weaned 21 days after birth and left undisturbed until adulthood (4 months). The study was conducted on male offspring rats only.

2.3. Behavioral analysis

Risk-taking behavior was assessed in the light/dark test (n=5 rats/group). The light/dark box apparatus consisted of two asymmetrical compartments: one dark compartment (5 lx; 30 × 32 × 32 cm;) and one light compartment (50 lx; 45 × 32 × 32 cm). A small opening (10 × 15 cm) connected the two compartments, thus enabling transition between the two boxes. The adult (4-month old) male PRS and control rats (n = 5 per group) were tested. Animals were housed in the testing room for 2 hours before the beginning of the test to enable adaptation to the new environment. The 5-minute test started when the animal was placed in the light compartment. A video camera located above the box recorded (1) the latency to the first spontaneous entry into the light compartment once the animal had entered the dark compartment, (2) the time spent in each compartment, and (3) the number of transitions to each compartment (data not shown). Scoring was performed by a trained observer using The Observer® (Noldus, The Netherlands). Of note, we used the term "risk-taking" behavior instead of "anxiety-like behavior" because, in our opinion, this term reflects the

nature of the behavioral test. “Anxiety” refers to a complex pathology in which a reduced risk-taking is only one aspect. Thus, we prefer to avoid the term “anxiety-like behavior” for a reduced risk-taking behavior in the light-dark test although we are aware that the test has pharmacological validity for the study of anxiolytic agents.

2.4. In situ hybridization

For gene imaging topography, radioactive *in situ* hybridization was performed according to previously published protocols (Ambesi-Impiombato et al., 2003). Animals (n=5 rats/group) were sacrificed by decapitation and their brains were immediately removed, frozen on powdered dry ice, and stored at -70°C to await sectioning. On a cryostat set at -18°C, serial coronal sections with a thickness of 12 µm were cut through the forebrain at the level of the medial prefrontal cortex (mPFC), the cortex and caudate putamen, the amygdala, and the hippocampus, with reference to the rat brain atlas by Paxinos and Watson (Paxinos and Watson 1997) (**Figure 1**). The sections were then thaw-mounted on to gelatin-coated slides and stored at -70°C for subsequent analysis. Radioactive *in situ* hybridization was carried out using oligodeoxyribonucleotide probes that were complementary with the mRNA sequences of the target genes (MWG Biotech, Italy) (**Table 1**); these were designed based on Gene-Bank sequences and checked using BLAST to avoid cross-hybridization. For each probe, a 50-µL labeling reaction mix was prepared on ice using DEPC-treated water, 1x tailing buffer, 7.5 pmol/µL of oligodeoxyribonucleotide, 125 units of terminal deoxynucleotidyl transferase (TdT), and 100 mCi 35^{S}-dATP. Unincorporated nucleotides were separated from radiolabeled DNA using ProbeQuant G-50 Micro Columns (Amersham-GE Healthcare Biosciences, Italy). Sections were fixed in 4% formaldehyde in 0.12-M PBS (pH 7.4), quickly rinsed three times with PBS, placed in 0.25% acetic anhydride in 0.1 M triethanolamine in 0.9% NaCl (pH 8.0) for 10 minutes, and then dehydrated in 70%, 80%, 95%, and 100% ethanol. The sections were then delipidated in chloroform for 5 minutes, rinsed again in 100% and 95% ethanol, and finally air-dried. Sections were hybridized using 0.4–0.6 x 106 of 2-cpm radiolabeled oligonucleotides in a buffer containing 50% formamide, 600 mM NaCl, 80 mM Tris-HCl (pH 4–7.5), 4 mM EDTA, 0.1% pyrophosphate, 0.2 mg/mL heparin sulfate, and 10% dextran-5 sulfate. The slides were incubated at 37°C in a humidified chamber for 22–24 hours and subsequently washed twice in SSC/50% formamide at 43ºC–44°C, and then once in SSC at room temperature. Finally, the sections were dried and exposed to a Kodak-10 Biomax MR autoradiographic film (Sigma, Italy); a slide containing a scale with 16 known amounts of ^{14}C (ARC-146C; American Radiolabeled Chemical) was co-exposed. The optimal exposure time was chosen to maximize signal-to-noise ratio, but to prevent the optical density from approaching the limits of saturation.

Quantitation of the autoradiographic signal was performed using a computerized image analysis system (ImageJ v. 1.46v; http://rsb.info.nih.gov/ij/). All hybridized sections used for comparative statistical analysis were exposed on the same sheet of X-ray film. Signal intensity analyses were carried out on digitized autoradiograms, and mean optical density was measured within outlined regions of interest (ROIs) in one or the other hemisphere for each section (**Figure 1**). Measurements of optical density within the ROIs were converted into relative dpm using a calibration curve based on the co-exposed standard scale; ^{14}C standard values from 4 through 12 were previously cross-calibrated to ^{35}S brain paste standards. To obtain a calibration curve for each X-ray film, a best fit 3rd degree polynomial was used. For each animal, measurements from four adjacent sections were averaged, and the final data were reported in relative dpm as mean ± SEM. The whole *in situ* hybridization procedure was performed blinded with coded frozen brains.

2.5. Statistical Analysis

Statistical analyses were performed using JMP9.0.1, SPSS 24.0, and Statistica software. One-way ANOVA (Group: control vs. PRS) was used to analyze behavior, while one-way ANOVA with repeated measures was used to analyze differences in gene expression, with region subdivisions used as within variables. Intergroup comparisons for one-way ANOVA and *post-hoc* analysis for two-way ANOVA (Group and Brain Region) were performed using the Newman–Keuls test. An independent-sample Student's t-test was performed to analyze differences in relative ratio gene expression levels between PRS and control rats. Correlation between behavioral data and gene expression levels was analyzed using Pearson's correlation analysis. Significance was set at $p < 0.05$.

3. Results

Gene expression topography

Homer1a

Statistically significant differences in *Homer1a* expression were found in different regions between the PRS and control animals. In particular, PRS up-regulated the transcript of *Homer1a* in both the basolateral amygdala (BLA) and the medial amygdala (MeA; **Figure 2**; Group effect: $F[1, 8] = 5.802$; $p < 0.05$), whereas it significantly reduced *Homer1a* mRNA levels in other brain regions, with differential effects in various subregions, including the dorsal hippocampus (**Figure 3**; Group effect: $F[3,24] = 45.071$; $p < 0.001$ and Group x region subdivisions effect: $F[3,24] = 4.020$; $p <$

0.05 for PRS vs. control, with the exception of the CA2 subdivision), the mPFC (**Figure 4;** Group effect: $F[1,8] = 9.668$; $p < 0.05$ and Group x region subdivisions effect: $F[5,40] = 2.5391$; $p < 0.05$ for PRS vs. control, with the exception of the lateral orbital cortex and secondary motor cortex subregions), the cortex (**Figure 5;** Group effect: $F[1,8] = 40.384$; $p < 0.001$ and Group x region subdivisions effect: $F[4,32] = 4.023$; $p < 0.001$ for PRS vs. control in all region subdivisions) and the caudate putamen–striatum (**Figure 5;** Group effect: $F[1,8] = 63.246$; $p < 0.001$).

Homer1b

No differences in *Homer1b* expression were found between PRS and control animals in any of the brain regions, with the exception of the BLA and MeA subdivisions of the amygdala (**Figure 2**), where PRS downregulated *Homer1b* expression (Group effect: $F[1,8] = 13.165$; $p < 0.001$).

mGlu5

Similar to *Homer1b*, mGlu5 mRNA levels were downregulated by PRS in the amygdala only, as shown in **Figure 2** (Group effect: $F[1,8] = 4.843$; $p < 0.05$). No differences were observed in the other brain regions.

Relative ratio of gene expression

The biological activity of the mGlu5-Homer1 system critically depends on the relative abundance of the two molecules (Kammermeier 2008). For this reason, we determined the ratio of normalized gene expression in PRS and control rats. As shown in **Figure 6**, *Homer1a* gene expression in PRS rats was normalized to expression in control rats and compared with either *Homer1b* or *Grm5* transcript expression. In the amygdala, *Homer1a* expression was higher in PRS rats than in control rats, while the opposite was true for *Homer1b* and *Grm5* transcripts. The relative expression of *Homer1a* was significantly higher than that of both *Homer1b* (Student's t-test: $t = 3.83$, $df = 1,8$; $p = 0.004$) and *Grm5* (Student's t-test: $t = 2.23$, $df = 1,8$; $p = 0.05$). In the dorsal hippocampus, expression of both *Homer1a* and *Homer1b* was higher in controls than in PRS rats, while expression of *Grm5* was predominant in PRS rats. A significant difference in relative expression between *Homer1a* and *Grm5* was found in the dorsal hippocampus (Student's t-test: $t = 2.43$, $df = 1,8$, $p = 0.04$). No differences were found between *Homer1a* and *Homer1b* in this regard. In all the other regions, expression of *Homer1a* was higher in controls than in PRS rats, and it was significantly lower than the relative expression of *Homer1b* and *Grm5* **(Figure 6).**

Risk-taking behavior

As shown in **Figure 7**, PRS rats showed reduced risk-taking behavior in the light/dark test, as indicated by the reduced time spent in the light box compared with the controls (Group effect: $F[1,8] = 28.383$, $p < 0.01$). The latency before the first spontaneous entry into the light box was higher in the controls than in the PRS rats (Group effect: $F[1,8] = 6.449$; $p < 0.05$; 54.5 ± 3.9 seconds *vs* 34.6 ± 6.8 seconds). No significant difference was found between the groups in terms of the number of light/dark transitions (data not shown).

Correlations between gene expression and risk-taking behavior

All PRS and control rats used in the topographical analysis of gene expression (n = 5 rats per group) had been previously tested for risk-taking behavior in the light/dark test. In each animal in each group, we examined the correlation between time spent in the light box and relative gene expression in each brain region and subdivision **(Figures 8–10)**. *Homer1a* expression was correlated with risk-taking behavior in all brain regions other than the cortex. In the amygdala, the correlation was negative (Pearson's correlation analysis, $r = -0.66$; $p < 0.05$), while in all other brain regions, we observed positive correlations (**Figures 9** and **10**). Behavior was positively correlated with *Homer1b* expression in the amygdala (**Figure 8**; Pearson's correlation analysis: $r = 0.81$; $p < 0.01$), cortex (**Figure 9B**; Pearson's correlation analysis: $r = 0.84$; $p < 0.01$), and caudate putamen-striatum (**Figure 10**). Behavior was positively correlated with *Grm5* expression in the amygdala (**Figure 8;** Pearson's correlation analysis: $r = 0.65$; $p < 0.05$) and in the cortex (**Figure 9C**; Pearson's correlation analysis: $r = 0.65$; $p < 0.05$).

4. Discussion

The goal of this study was to evaluate whether exposure to perinatal stress can shape synapse architecture at the postsynaptic level and in different brain regions linked to stress and stress-prone behavioral disorders; in this way, we aimed to expand and complete our previous data of impaired presynaptic architecture (Mairesse et al., 2015, Mairesse et al., 2012, Marrocco et al., 2012, Marrocco et al., 2014). To this end, we specifically focused on the genes encoding the mGlu5 and Homer proteins because the mGlu5 play a role in resilience to stress (Shin et al., 2015; Wagner et al., 2015; Sun et al., 2017; Schwendt et al., 2018; Yim et al., 2018).

We found that PRS affected the expression patterns of *Homer1a, Homer1b*, and *Grm5* in the central nervous system. A major finding was that the expression pattern of the three genes differed between the amygdala and all other regions examined, with PRS enhancing *Homer1a* expression exclusively in the amygdala. In contrast, *Grm5* and *Homer1b* expression were higher than *Homer1a* expression in all other brain regions. Homer1a is the product of an immediate early gene and acts as a master regulator of mGlu5 function. Up-regulation of Homer1a disrupts mGlu5-Homer1b, interactions, thereby restraining all signaling mechanisms that rely on long Homer-mediated protein-to-protein interaction, such as intracellular Ca^{2+} mobilization (Mao et al., 2005, Roche et al., 1999).

These findings may have important implications for our understanding of the role played by different brain regions in the overall response to stress. The positive ratio between Homer1a and mGlu5/Homer1b in the amygdala suggests that PRS causes long-lasting impairment of canonical mGlu5 signaling—i.e., coupling between mGlu5 activation and intracellular Ca^{2+} mobilization resulting from local activation of InsP3 receptors. This might favor mGlu5 signaling via Homer-independent mechanisms, such as the opening of voltage-sensitive Ca^{2+} channels, or arrestin-dependent activation of MAP kinase or phosphatidylinositol-3-kinase pathway during receptor desensitization and internalization. The opposite scenario may take place in the other brain regions, where expression of the genes encoding Homer1b and mGlu5 was greater than that of the genes encoding Homer1a in PRS rats.

Another interesting finding was the correlation between changes in *Grm5/Homer* expression and behavioral abnormalities in PRS rats. Specifically, PRS rats spent less time in the light box than unstressed controls, confirming the characteristic phenotype of reduced risk-taking behavior previously observed in the PRS rat model (Marrocco et al., 2012, Morley-Fletcher et al., 2011, Zuena et al., 2008). Interestingly, we found that *Homer1a* expression in the amygdala was inversely correlated with time spent in the light compartment of the light/dark box, and that expression of *Homer1b* and *Grm5* was positively correlated. In contrast, in most subregions of the dorsal

hippocampus, mPFC, and neostriatum, *Homer1a* gene expression was positively correlated with time spent in the light compartment.

The amygdala is one of the brain regions most involved in stress-related disorders, and its over-activation (Shin and Liberzon, 2010) combined with *Homer1a* overexpression (Mahan et al., 2012), play a central role in fear conditioning. Accordingly, *Homer1a* knockout mice showed impaired long-term fear memory formation (Inoue et al., 2009). With regards to the present study, the increased *Homer1a* expression found in the amygdala of PRS rats suggests that these rats are more prone to developing fear memory in response to stress, which is consistent with the reduced risk-taking behavior. Moreover, because *Homer1a* expression is a marker for neuronal depolarization (Hu et al., 2010), persistent overexpression of *Homer1a* in the amygdala of PRS rats may reflect sustained neuronal activation in this region, which is associated with stress-related behaviors (Ressler 2010). Indeed, we have previously shown increased neuronal reactivity in the amygdala in PRS rats (Mairesse et al., 2007). In addition, the present data indicate that PRS modulates the mGlu5-Homer1 interaction, corroborating previous data on Homer1a and Homer1b at the transcript and protein levels in different animal models of stress (Ary et al., 2007, Wagner et al., 2015).

We were surprised to find that PRS significantly reduced *Homer1a* mRNA levels in the dorsal hippocampus, because hippocampal *Homer1a* expression is markedly increased in all hippocampus regions in response to acute stress (Clifton et al., 2017, Qi et al., 2010). In contrast, overexpression of Homer1b/c in the dorsal hippocampus reduces the impairment of spatial object recognition in mice exposed to social defeat stress (Wagner et al., 2013). One possible explanation for our findings is that reduced Homer1a expression in the dorsal hippocampus and other brain regions of PRS rats represents a defensive mechanism that supports canonical mGlu5/Homer1b/c signaling, thereby avoiding robust abnormalities in activity-dependent synaptic plasticity, spatial memory, and cognitive function in animals exposed to early life stress. Therefore, region-specific *Homer1a* expression and its impact on mGlu5-Homer1b/c *vs.* mGlu5-Homer1a signaling may shape the vulnerability of stress-related brain regions to early life events. This influences the developmental trajectory of the hypothalamic–pituitary–adrenal axis and the brain response to stress in the adult life.

In conclusion, the results of gene expression mapping in the present study, as well as the correlation between gene expression and behavior in PRS rats, show that early life events critically influence PSD molecules, which control excitatory synaptic responses and the induction and expression of long-term mechanisms of synaptic plasticity. Overall, the PRS integrated model might be of great

value in deciphering the mechanisms of resilience to stress and unraveling the intricate mechanisms that lie at the border between the physiological and pathological responses to stress.

Role of the funding sources

This work was partially supported by the Department of Neuroscience, Reproductive and Odontostomatological Sciences, University Federico II of Naples, Italy, through its own research-devoted funding to the Laboratory of Molecular Psychiatry (Andrea de Bartolomeis). This study was also supported by the University of Lille, Sapienza University of Rome (Framework Agreement signed on February 15th, 2007), and the CNRS within the framework of the Prenatal Stress and Neurodegenerative Diseases International Associated Laboratory (LIA-PSND), co-directed by Professors S. Maccari (France) and F. Nicoletti (Italy). Behavioral assessments were carried out using the platform PHExMAR of the University of Lille. We are indebted to the Research Federation FRABio (Univ. Lille, CNRS, FR 3688, FRABio, Biochimie Structurale et Fonctionnelle des Assemblages Biomoléculaires) for providing the scientific and technical environment conducive to completing this body of work.

English editing was provided by Editing Elsevier services.

Declaration of interest

None. The funding source had no role in the study design, in the collection, analysis, and interpretation of data, in the writing of the report, and in the decision to submit the article for publication.

Figure Legends

Figure 1. Regions of interest for topographical evaluation of gene expression. Medial prefrontal cortex (MO: medial orbital cortex, VO: ventral orbital cortex, LO: lateral orbital cortex, AI: agranular insular cortex, M2: secondary motor cortex, Prl: prelimbic cortex). Amygdala (BLA: basolateral amygdala, MeA: medial amygdala). Cortex and caudate putamen (ACC: anterior cingulate cortex, MAC: medial agranular cortex (premotor cortex), MC: motor cortex, SS: somatosensory cortex, IC: insular cortex, DM: dorsomedial putamen, DL: dorsolateral putamen, VM: ventromedial putamen, VL: ventrolateral putamen, Cab: core of the nucleus accumbens, Sab: shell of the nucleus accumbens). Dorsal hippocampus (DG: dentate gyrus, CA1, CA2, CA3 Ammon's Corn).

Figure 2. Autoradiographic film images of *Homer1a, Homer1b,* and *mGlu5* mRNAs detected using *in situ* hybridization histochemistry in coronal brain sections at the level of amygdala in PRS and control (CONT) rats n=5/group. Levels of mRNA expression are in relative dpm. Values are expressed as means ± SEM *$p < 0.05$ compared with control.

Figure 3. Autoradiographic film images of *Homer1a, Homer1b,* and *mGlu5* mRNA detected using *in situ* hybridization histochemistry in coronal brain sections at the level of the dorsal hippocampus in PRS and control (CONT) rats (n=5 per group). Levels of mRNA expression are in relative dpm. Values are expressed as means ± SEM. **$p < 0.001$ compared with control.

Figure 4. Autoradiographic film images of *Homer1a, Homer1b and mGlu5* mRNAs detected by means of *in situ* hybridization histochemistry in coronal brain sections at the level of medial Prefrontal Cortex in PRS and control (CONT) unstressed rats (n=5 per group). Levels of mRNA expression are in relative dpm. Values are expressed as means ± SEM. ** $p < 0.001$ compared with control.

Figure 5. Autoradiographic film images of *Homer1a, Homer1b,* and *mGlu5* mRNAs detected using *in situ* hybridization histochemistry in coronal brain sections at the level of the cortex and caudate putamen in PRS and control (CONT) rats (n=5 per group). Levels of mRNA expression are in relative dpm. Values are expressed as means ± SEM. **$p < 0.001$ compared with control.

Figure 6. Relative ratio of *Homer1a vs. Homer1b* (upper panel) and of *Homer1a vs. mGlu5* (lower panel) mRNA expression in outlined regions of interest (Amy: amygdala, dHPC: dorsal hippocampus, CP: caudate putamen). For each brain region, *Homer1a* gene expression in PRS rats was normalized to expression in the control group and compared with either *Homer1b* or *mGlu5*

transcripts. A ratio > 1 indicates higher gene expression in PRS rats, while a ratio < 1 indicates lower gene expression in PRS rats. *p < 0.05.

Figure 7. Risk-taking behavior in the light/dark test in PRS and control (CONT) unstressed rats (n=5 per group). Both time spent in the light box (left) and latency to enter the light box (right) were reduced by PRS. Values are expressed as means ± SEM. * p < 0.05 compared with control.

Figures 8. Correlations between risk-taking behavior and gene expression in the amygdala
Pearson's correlation analyses between time spent in the light box of the light/dark test and relative dpm for *Homer1a, Homer1b,* and *mGlu5* in PRS and control (CONT) rats.

Figures 9. Correlations between risk-taking behavior and gene expression in each region of interest
Pearson's correlation analyses between time spent in the light box of the light/dark test and relative dpm for *Homer1a* in medial prefrontal cortex (A) and dorsal hippocampus (D-F) in PRS and control (CONT) rats. B and C: Pearson's correlation analyses between time spent in the light box of the light/dark test and relative dpm for *Homer1b,* and *mGlu5* in PRS and control (CONT) rats.

Figures 10. **Correlations between risk-taking behavior and gene expression in striatum**
Pearson's correlation analyses between time spent in the light box of the light/dark test and relative dpm for *Homer1a, Homer1b,* and *mGlu5* in PRS and control (CONT) rats.

References

Alonso J, Lepine JP, Committee ESMS. Overview of key data from the European Study of the Epidemiology of Mental Disorders (ESEMeD). J Clin Psychiatry. 2007;68 Suppl 2:3-9.

Ambesi-Impiombato A, D'Urso G, Muscettola G, de Bartolomeis A. Method for quantitative in situ hybridization histochemistry and image analysis applied for Homer1a gene expression in rat brain. Brain Res Brain Res Protoc. 2003;11:189-96.

Ango F, Prezeau L, Muller T, Tu JC, Xiao B, Worley PF, et al. Agonist-independent activation of metabotropic glutamate receptors by the intracellular protein Homer. Nature. 2001;411:962-5.

Ary AW, Aguilar VR, Szumlinski KK, Kippin TE. Prenatal stress alters limbo-corticostriatal Homer protein expression. Synapse. 2007;61:938-41.

Bagley J, Moghaddam B. Temporal dynamics of glutamate efflux in the prefrontal cortex and in the hippocampus following repeated stress: effects of pretreatment with saline or diazepam. Neuroscience. 1997;77:65-73.

Barker DJ, Bagby SP, Hanson MA. Mechanisms of disease: in utero programming in the pathogenesis of hypertension. Nat Clin Pract Nephrol. 2006;2:700-7.

Bertaso F, Roussignol G, Worley P, Bockaert J, Fagni L, Ango F. Homer1a-dependent crosstalk between NMDA and metabotropic glutamate receptors in mouse neurons. PLoS One. 2010;5:e9755.

Brakeman PR, Lanahan AA, O'Brien R, Roche K, Barnes CA, Huganir RL, et al. Homer: a protein that selectively binds metabotropic glutamate receptors. Nature. 1997;386:284-8.

Buonaguro EF, Iasevoli F, Marmo F, Eramo A, Latte G, Avagliano C, et al. Re-arrangements of gene transcripts at glutamatergic synapses after prolonged treatments with antipsychotics: A putative link with synaptic remodeling. Prog Neuropsychopharmacol Biol Psychiatry. 2017a;76:29-41.

Buonaguro EF, Tomasetti C, Chiodini P, Marmo F, Latte G, Rossi R, et al. Postsynaptic density protein transcripts are differentially modulated by minocycline alone or in add-on to haloperidol: Implications for treatment resistant schizophrenia. J Psychopharmacol. 2017b;31:406-17.

Chen Q, Tang M, Mamiya T, Im HI, Xiong X, Joseph A, et al. Bi-directional effect of cholecystokinin receptor-2 overexpression on stress-triggered fear memory and anxiety in the mouse. PLoS One. 2010;5:e15999.

Clifton NE, Cameron D, Trent S, Sykes LH, Thomas KL, Hall J. Hippocampal Regulation of Postsynaptic Density Homer1 by Associative Learning. Neural Plast. 2017;2017:5959182.

Collins MO, Husi H, Yu L, Brandon JM, Anderson CN, Blackstock WP, et al. Molecular characterization and comparison of the components and multiprotein complexes in the postsynaptic proteome. J Neurochem. 2006;97 Suppl 1:16-23.

Danysz W, Zajaczkowski W, Parsons CG. Modulation of learning processes by ionotropic glutamate receptor ligands. Behav Pharmacol. 1995;6:455-74.

de Bartolomeis A, Buonaguro EF, Latte G, Rossi R, Marmo F, Iasevoli F, et al. Immediate-Early Genes Modulation by Antipsychotics: Translational Implications for a Putative Gateway to Drug-Induced Long-Term Brain Changes. Front Behav Neurosci. 2017;11:240.

de Bartolomeis A, Fiore G, Iasevoli F. Dopamine-glutamate interaction and antipsychotics mechanism of action: implication for new pharmacological strategies in psychosis. Curr Pharm Des. 2005;11:3561-94.

de Bartolomeis A, Marmo F, Buonaguro EF, Latte G, Tomasetti C, Iasevoli F. Switching antipsychotics: Imaging the differential effect on the topography of postsynaptic density transcripts in antipsychotic-naive vs. antipsychotic-exposed rats. Prog Neuropsychopharmacol Biol Psychiatry. 2016;70:24-38.

de Bartolomeis A, Marmo F, Buonaguro EF, Rossi R, Tomasetti C, Iasevoli F. Imaging brain gene expression profiles by antipsychotics: region-specific action of amisulpride on postsynaptic density transcripts compared to haloperidol. Eur Neuropsychopharmacol. 2013;23:1516-29.

de Bartolomeis A, Tomasetti C. Calcium-dependent networks in dopamine-glutamate interaction: the role of postsynaptic scaffolding proteins. Mol Neurobiol. 2012;46:275-96.

Gold MG. A frontier in the understanding of synaptic plasticity: solving the structure of the postsynaptic density. Bioessays. 2012;34:599-608.

Hu JH, Park JM, Park S, Xiao B, Dehoff MH, Kim S, et al. Homeostatic scaling requires group I mGluR activation mediated by Homer1a. Neuron. 2010;68:1128-42.

Iasevoli F, Buonaguro EF, Sarappa C, Marmo F, Latte G, Rossi R, et al. Regulation of postsynaptic plasticity genes' expression and topography by sustained dopamine perturbation and modulation by acute memantine: relevance to schizophrenia. Prog Neuropsychopharmacol Biol Psychiatry. 2014;54:299-314.

Inoue N, Nakao H, Migishima R, Hino T, Matsui M, Hayashi F, et al. Requirement of the immediate early gene vesl-1S/homer-1a for fear memory formation. Mol Brain. 2009;2:7.

Jia N, Li Q, Sun H, Song Q, Tang G, Sun Q, et al. Alterations of Group I mGluRs and BDNF Associated with Behavioral Abnormity in Prenatally Stressed Offspring Rats. Neurochem Res. 2015;40:1074-82.

Kammermeier PJ. Endogenous homer proteins regulate metabotropic glutamate receptor signaling in neurons. J Neurosci. 2008;28:8560-7.

Laloux C, Mairesse J, Van Camp G, Giovine A, Branchi I, Bouret S, et al. Anxiety-like behaviour and associated neurochemical and endocrinological alterations in male pups exposed to prenatal stress. Psychoneuroendocrinology. 2012;37:1646-58.

Lepine JP. The epidemiology of anxiety disorders: prevalence and societal costs. J Clin Psychiatry. 2002;63 Suppl 14:4-8.

Lum JS, Fernandez F, Matosin N, Andrews JL, Huang XF, Ooi L, et al. Neurodevelopmental Expression Profile of Dimeric and Monomeric Group 1 mGluRs: Relevance to Schizophrenia Pathogenesis and Treatment. Sci Rep. 2016;6:34391.

Luoni A, Berry A, Calabrese F, Capoccia S, Bellisario V, Gass P, et al. Delayed BDNF alterations in the prefrontal cortex of rats exposed to prenatal stress: preventive effect of lurasidone treatment during adolescence. Eur Neuropsychopharmacol. 2014;24:986-95.

Maccari S, Krugers HJ, Morley-Fletcher S, Szyf M, Brunton PJ. The consequences of early-life adversity: neurobiological, behavioural and epigenetic adaptations. J Neuroendocrinol. 2014;26:707-23.

Maccari S, Piazza PV, Kabbaj M, Barbazanges A, Simon H, Le Moal M. Adoption reverses the long-term impairment in glucocorticoid feedback induced by prenatal stress. J Neurosci. 1995;15:110-6.

Mahan AL, Mou L, Shah N, Hu JH, Worley PF, Ressler KJ. Epigenetic modulation of Homer1a transcription regulation in amygdala and hippocampus with pavlovian fear conditioning. J Neurosci. 2012;32:4651-9.

Mairesse J, Gatta E, Reynaert ML, Marrocco J, Morley-Fletcher S, Soichot M, et al. Activation of presynaptic oxytocin receptors enhances glutamate release in the ventral hippocampus of prenatally restraint stressed rats. Psychoneuroendocrinology. 2015;62:36-46.

Mairesse J, Vercoutter-Edouart AS, Marrocco J, Zuena AR, Giovine A, Nicoletti F, et al. Proteomic characterization in the hippocampus of prenatally stressed rats. J Proteomics. 2012;75:1764-70.

Mairesse J, Viltart O, Salome N, Giuliani A, Catalani A, Casolini P, et al. Prenatal stress alters the negative correlation between neuronal activation in limbic regions and behavioral responses in rats exposed to high and low anxiogenic environments. Psychoneuroendocrinology. 2007;32:765-76.

Mao L, Yang L, Tang Q, Samdani S, Zhang G, Wang JQ. The scaffold protein Homer1b/c links metabotropic glutamate receptor 5 to extracellular signal-regulated protein kinase cascades in neurons. J Neurosci. 2005;25:2741-52.

Marrocco J, Mairesse J, Ngomba RT, Silletti V, Van Camp G, Bouwalerh H, et al. Anxiety-like behavior of prenatally stressed rats is associated with a selective reduction of glutamate release in the ventral hippocampus. J Neurosci. 2012;32:17143-54.

Marrocco J, Reynaert ML, Gatta E, Gabriel C, Mocaer E, Di Prisco S, et al. The effects of antidepressant treatment in prenatally stressed rats support the glutamatergic hypothesis of stress-related disorders. J Neurosci. 2014;34:2015-24.

Moghaddam B. Stress activation of glutamate neurotransmission in the prefrontal cortex: implications for dopamine-associated psychiatric disorders. Biol Psychiatry. 2002;51:775-87.

Morley-Fletcher S, Mairesse J, Soumier A, Banasr M, Fagioli F, Gabriel C, et al. Chronic agomelatine treatment corrects behavioral, cellular, and biochemical abnormalities induced by prenatal stress in rats. Psychopharmacology (Berl). 2011;217:301-13.

Morley-Fletcher S, Rea M, Maccari S, Laviola G. Environmental enrichment during adolescence reverses the effects of prenatal stress on play behaviour and HPA axis reactivity in rats. Eur J Neurosci. 2003;18:3367-74.

Morley-Fletcher S, Zuena AR, Mairesse J, Gatta E, Van Camp G, Bouwalerh H, et al. The reduction in glutamate release is predictive of cognitive and emotional alterations that are corrected by the positive modulator of AMPA receptors S 47445 in perinatal stressed rats. Neuropharmacology. 2018;135:284-96.

Musazzi L, Treccani G, Mallei A, Popoli M. The action of antidepressants on the glutamate system: regulation of glutamate release and glutamate receptors. Biol Psychiatry. 2013;73:1180-8.

Palmfeldt J, Henningsen K, Eriksen SA, Muller HK, Wiborg O. Protein biomarkers of susceptibility and resilience to stress in a rat model of depression. Mol Cell Neurosci. 2016;74:87-95.

Paxinos G, Watson C. The Rat Brain in Stereotaxic Coordinates. Sidney, Australia: Academic Press Inc.; 1997.

Popoli M, Yan Z, McEwen BS, Sanacora G. The stressed synapse: the impact of stress and glucocorticoids on glutamate transmission. Nat Rev Neurosci. 2011;13:22-37.

Qi C, Roseboom PH, Nanda SA, Lane JC, Speers JM, Kalin NH. Anxiety-related behavioral inhibition in rats: a model to examine mechanisms underlying the risk to develop stress-related psychopathology. Genes Brain Behav. 2010;9:974-84.

Ressler KJ. Amygdala activity, fear, and anxiety: modulation by stress. Biol Psychiatry. 2010;67:1117-9.

Robbins TW, Murphy ER. Behavioural pharmacology: 40+ years of progress, with a focus on glutamate receptors and cognition. Trends Pharmacol Sci. 2006;27:141-8.

Roche KW, Tu JC, Petralia RS, Xiao B, Wenthold RJ, Worley PF. Homer 1b regulates the trafficking of group I metabotropic glutamate receptors. J Biol Chem. 1999;274:25953-7.

Serchov T, Heumann R, van Calker D, Biber K. Signaling pathways regulating Homer1a expression: implications for antidepressant therapy. Biol Chem. 2016;397:207-14.

Shcheglovitov A, Shcheglovitova O, Yazawa M, Portmann T, Shu R, Sebastiano V, et al. SHANK3 and IGF1 restore synaptic deficits in neurons from 22q13 deletion syndrome patients. Nature. 2013;503:267-71.

Sheng M, Hoogenraad CC. The postsynaptic architecture of excitatory synapses: a more quantitative view. Annu Rev Biochem. 2007;76:823-47.

Shin LM, Liberzon I. The neurocircuitry of fear, stress, and anxiety disorders. Neuropsychopharmacology. 2010;35:169-91.

Shin S, Kwon O, Kang JI, Kwon S, Oh S, Choi J, Kim CH, Kim DG. mGlu5 in the nucleus accumbens is critical for promoting resilience to chronic stress. Nat Neurosci. 2015 Jul;18(7):1017-24. doi: 10.1038/nn.4028.

Schwendt M, Shallcross J, Hadad NA, Namba MD, Hiller H, Wu L, Krause EG, Knackstedt LA. A novel rat model of comorbid PTSD and addiction reveals intersections between stress susceptibility and enhanced cocaine seeking with a role for mGlu5 receptors. Transl Psychiatry. 2018 Oct 5;8(1):209. doi: 10.1038/s41398-018-0265-9.

Soler J, Fananas L, Parellada M, Krebs MO, Rouleau GA, Fatjo-Vilas M. Genetic variability in scaffolding proteins and risk for schizophrenia and autism-spectrum disorders: a systematic review. J Psychiatry Neurosci. 2018;43:223-44.

Sun H, Su R, Zhang X, Wen J, Yao D, Gao X, Zhu Z, Li H. Hippocampal GR- and CB1-mediated mGlu5 differentially produces susceptibility and resilience to acute and chronic mild stress in rats. Neuroscience. 2017 Aug 15;357:295-302. doi: 10.1016/j.neuroscience.2017.06.017.

Sun L, Gooding HL, Brunton PJ, Russell JA, Mitchell R, Fleetwood-Walker S. Phospholipase D-mediated hypersensitivity at central synapses is associated with abnormal behaviours and pain sensitivity in rats exposed to prenatal stress. Int J Biochem Cell Biol. 2013;45:2706-12.

Tu JC, Xiao B, Naisbitt S, Yuan JP, Petralia RS, Brakeman P, et al. Coupling of mGluR/Homer and PSD-95 complexes by the Shank family of postsynaptic density proteins. Neuron. 1999;23:583-92.

Tu JC, Xiao B, Yuan JP, Lanahan AA, Leoffert K, Li M, et al. Homer binds a novel proline-rich motif and links group 1 metabotropic glutamate receptors with IP3 receptors. Neuron. 1998;21:717-26.

Vyas A, Mitra R, Shankaranarayana Rao BS, Chattarji S. Chronic stress induces contrasting patterns of dendritic remodeling in hippocampal and amygdaloid neurons. J Neurosci. 2002;22:6810-8.

Wagner KV, Hartmann J, Labermaier C, Hausl AS, Zhao G, Harbich D, et al. Homer1/mGlu5 activity moderates vulnerability to chronic social stress. Neuropsychopharmacology. 2015;40:1222-33.

Wagner KV, Hartmann J, Mangold K, Wang XD, Labermaier C, Liebl C, et al. Homer1 mediates acute stress-induced cognitive deficits in the dorsal hippocampus. J Neurosci. 2013;33:3857-64.

Yim YS, Han W, Seo J, Kim CH, Kim DG. Differential mGlu5 expression in response to the same stress causes individually adapted hippocampal network activity. Biochem Biophys Res Commun. 2018 Jan 1;495(1):1305-1311. doi: 10.1016/j.bbrc.2017.11.172.

Yuan JP, Kiselyov K, Shin DM, Chen J, Shcheynikov N, Kang SH, et al. Homer binds TRPC family channels and is required for gating of TRPC1 by IP3 receptors. Cell. 2003;114:777-89.

Yuen EY, Liu W, Karatsoreos IN, Feng J, McEwen BS, Yan Z. Acute stress enhances glutamatergic transmission in prefrontal cortex and facilitates working memory. Proc Natl Acad Sci U S A. 2009;106:14075-9.

Zhang XH, Jia N, Zhao XY, Tang GK, Guan LX, Wang D, et al. Involvement of pGluR1, EAAT2 and EAAT3 in offspring depression induced by prenatal stress. Neuroscience. 2013;250:333-41.

Zuena AR, Mairesse J, Casolini P, Cinque C, Alema GS, Morley-Fletcher S, et al. Prenatal restraint stress generates two distinct behavioral and neurochemical profiles in male and female rats. PLoS One. 2008;3:e2170.

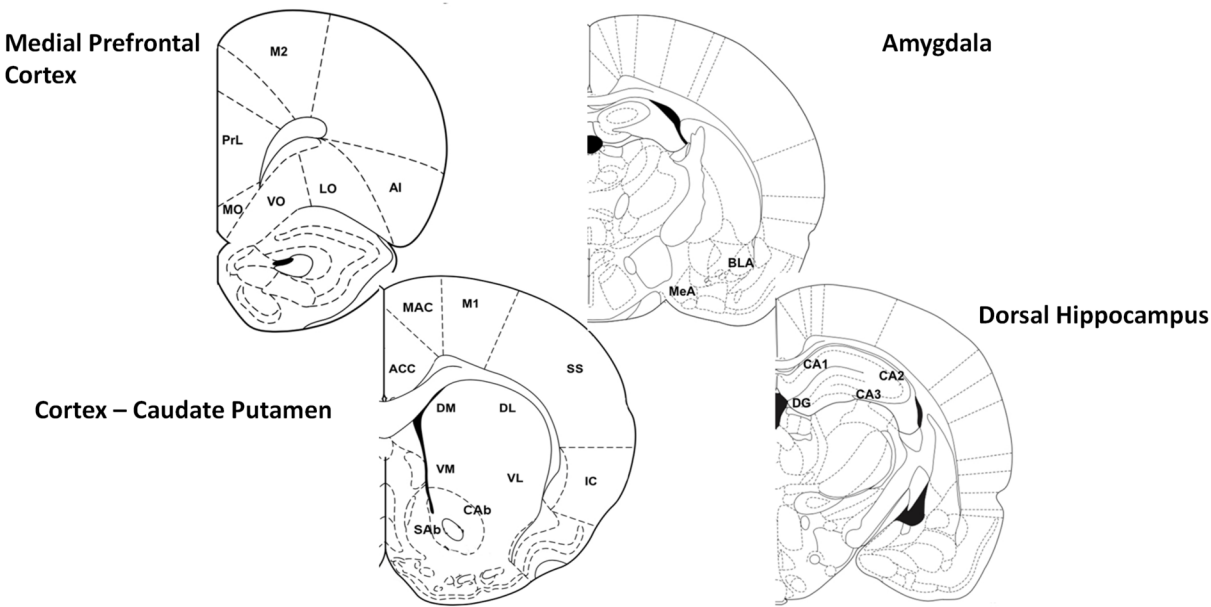
Medial Prefrontal Cortex
M2
PrL
MO
VO
LO
AI
Amygdala
BLA
MeA
Dorsal Hippocampus
CA1
CA2
CA3
DG
Cortex – Caudate Putamen
MAC
M1
ACC
SS
DM
DL
VM
VL
IC
CAb
SAb

Figure 1

mRNA expression in Amygdala

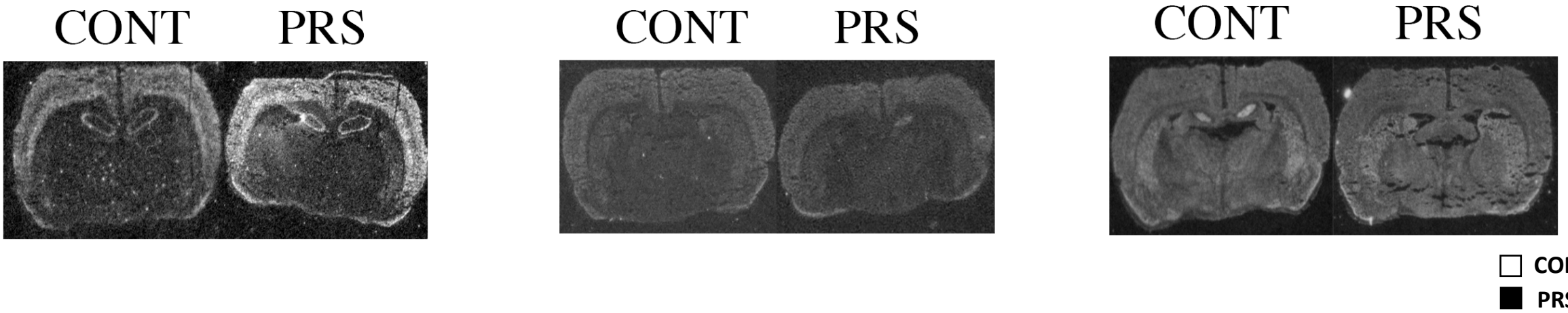

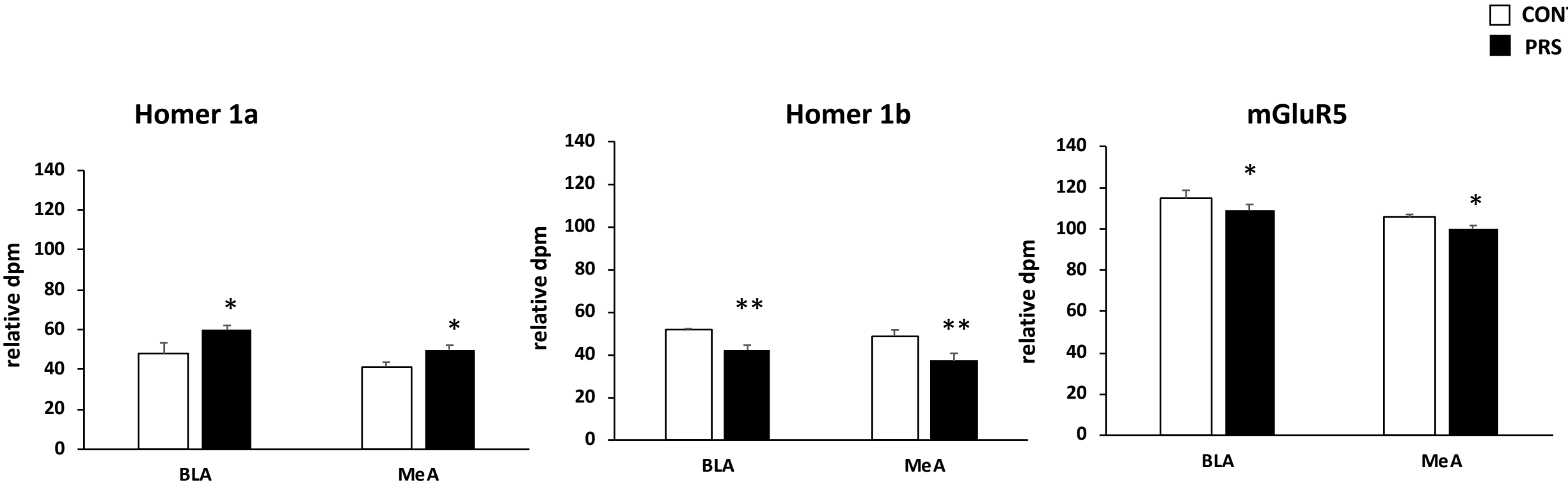

Figure 2

mRNA expression in dorsal Hippocampus

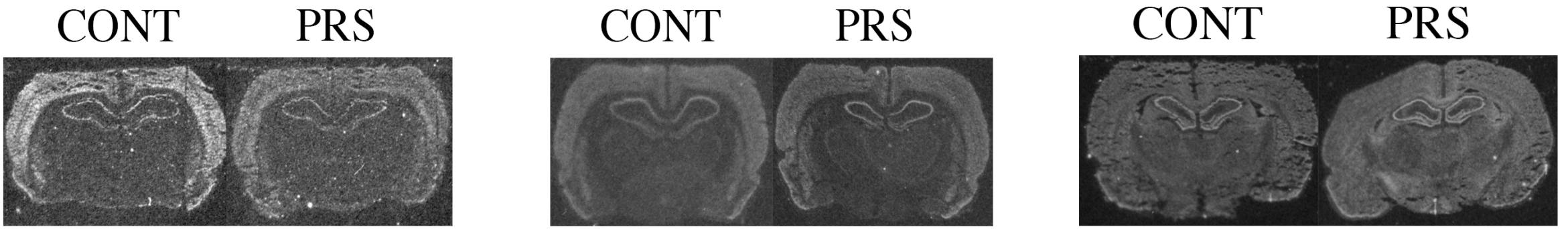

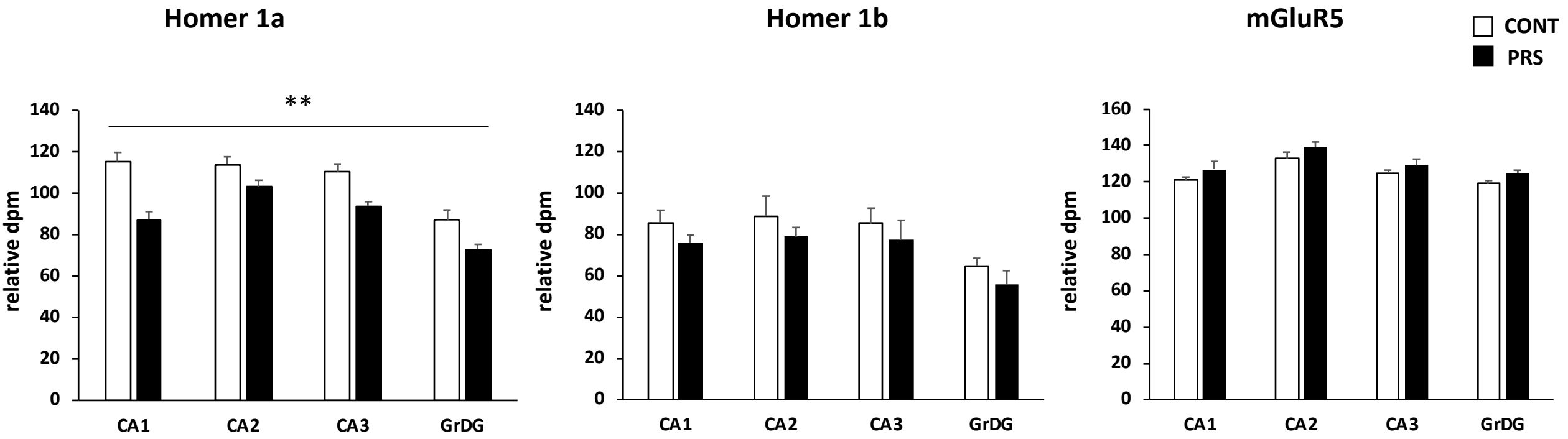

Figure 3

mRNA expression in Medial Prefrontal Cortex

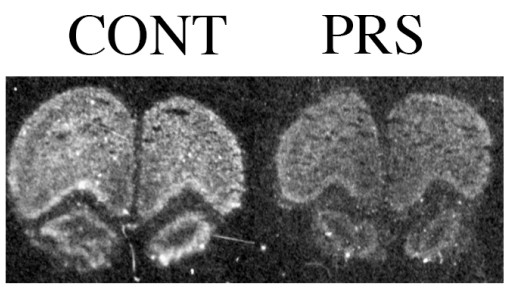

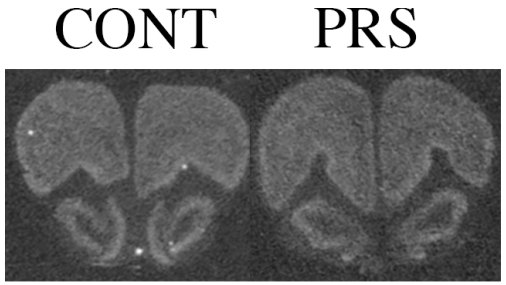

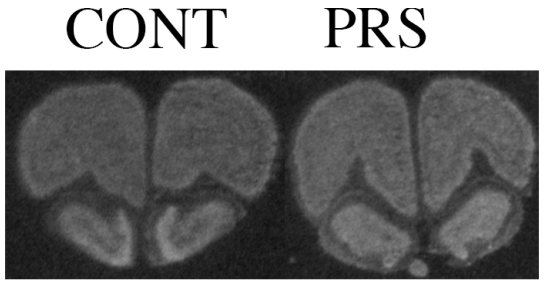

CONT
PRS

Homer 1a

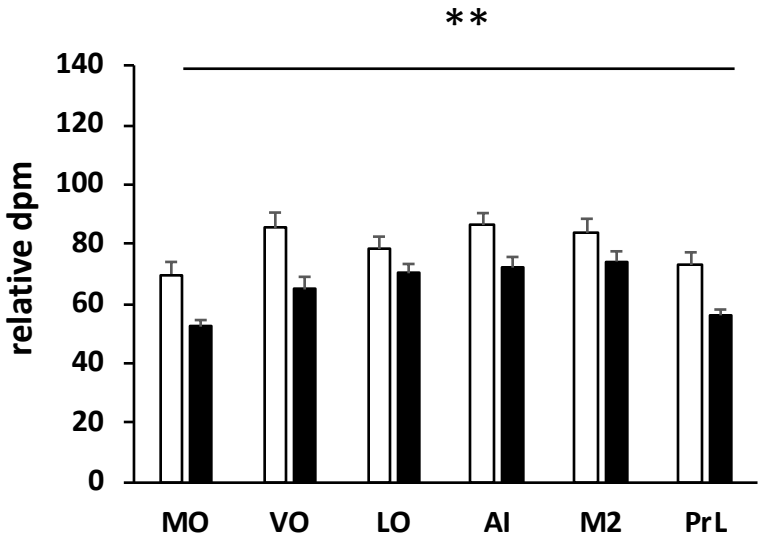

Homer 1b

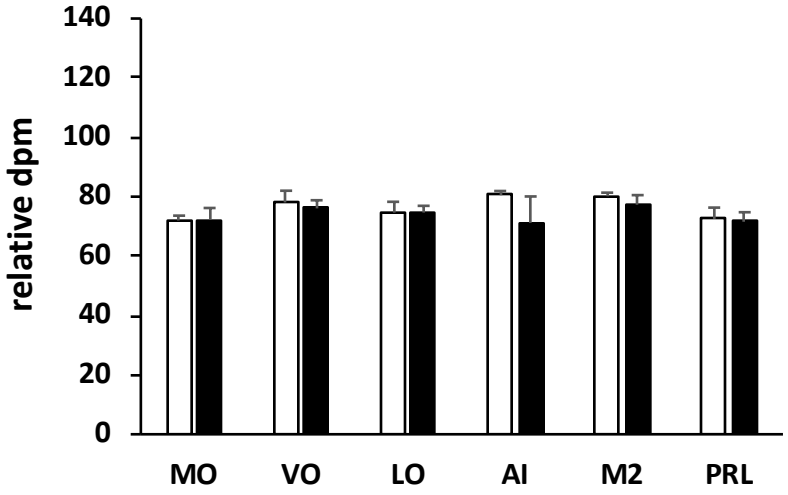

mGluR5

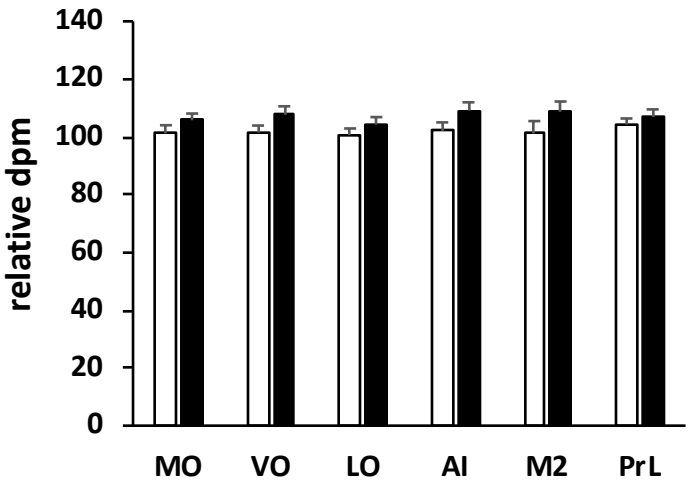

Figure 4

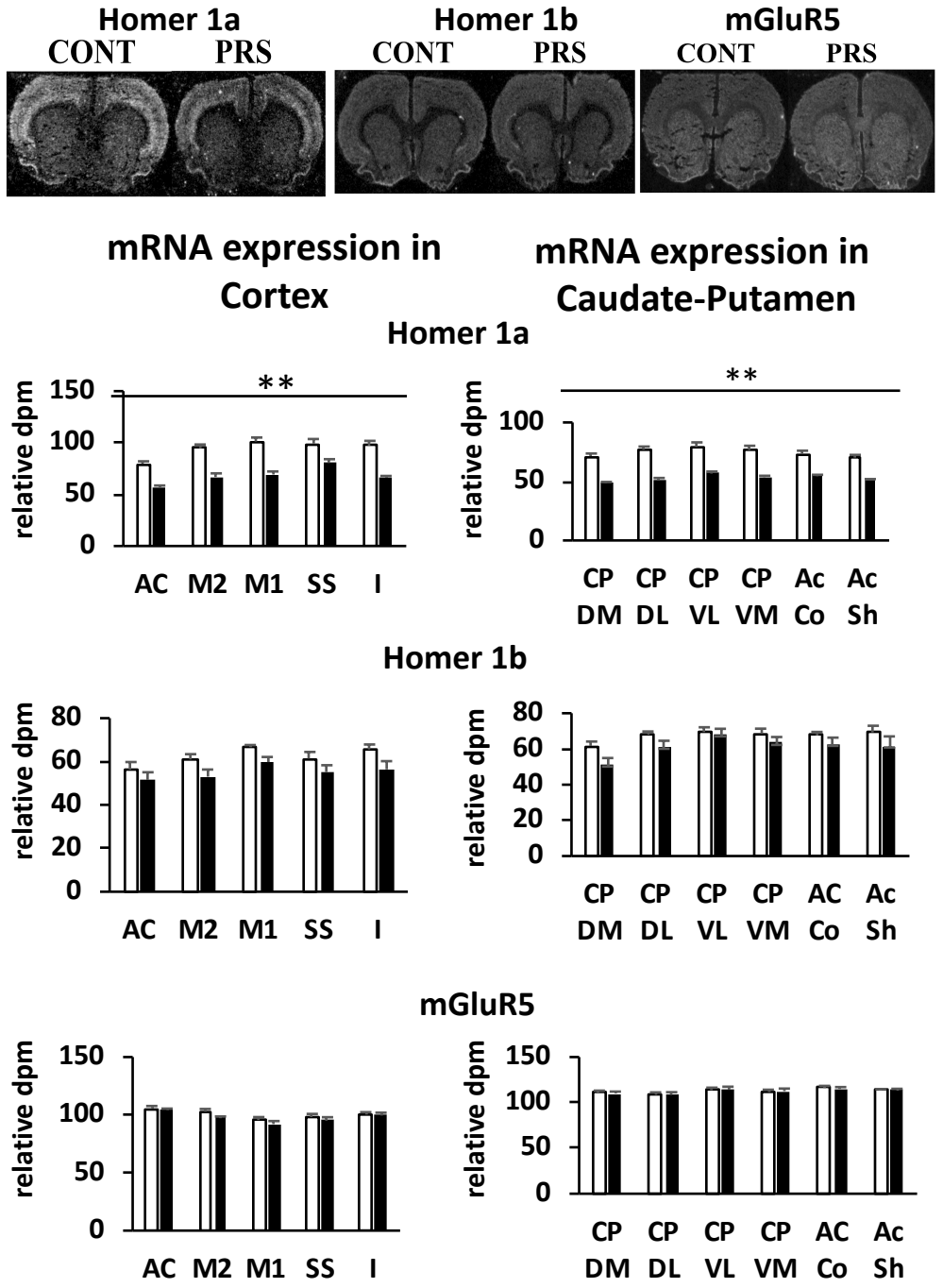
Homer 1a
CONT
PRS
Homer 1b
CONT
PRS
mGluR5
CONT
PRS
mRNA expression in Cortex
mRNA expression in Caudate-Putamen
Homer 1a
relative dpm
150
100
50
0
**
AC
M2
M1
SS
I
relative dpm
100
50
0
**
CP DM
CP DL
CP VL
CP VM
Ac Co
Ac Sh
Homer 1b
relative dpm
80
60
40
20
0
AC
M2
M1
SS
I
relative dpm
80
60
40
20
0
CP DM
CP DL
CP VL
CP VM
AC Co
Ac Sh
mGluR5
relative dpm
150
100
50
0
AC
M2
M1
SS
I
relative dpm
150
100
50
0
CP DM
CP DL
CP VL
CP VM
AC Co
Ac Sh

Figure 5

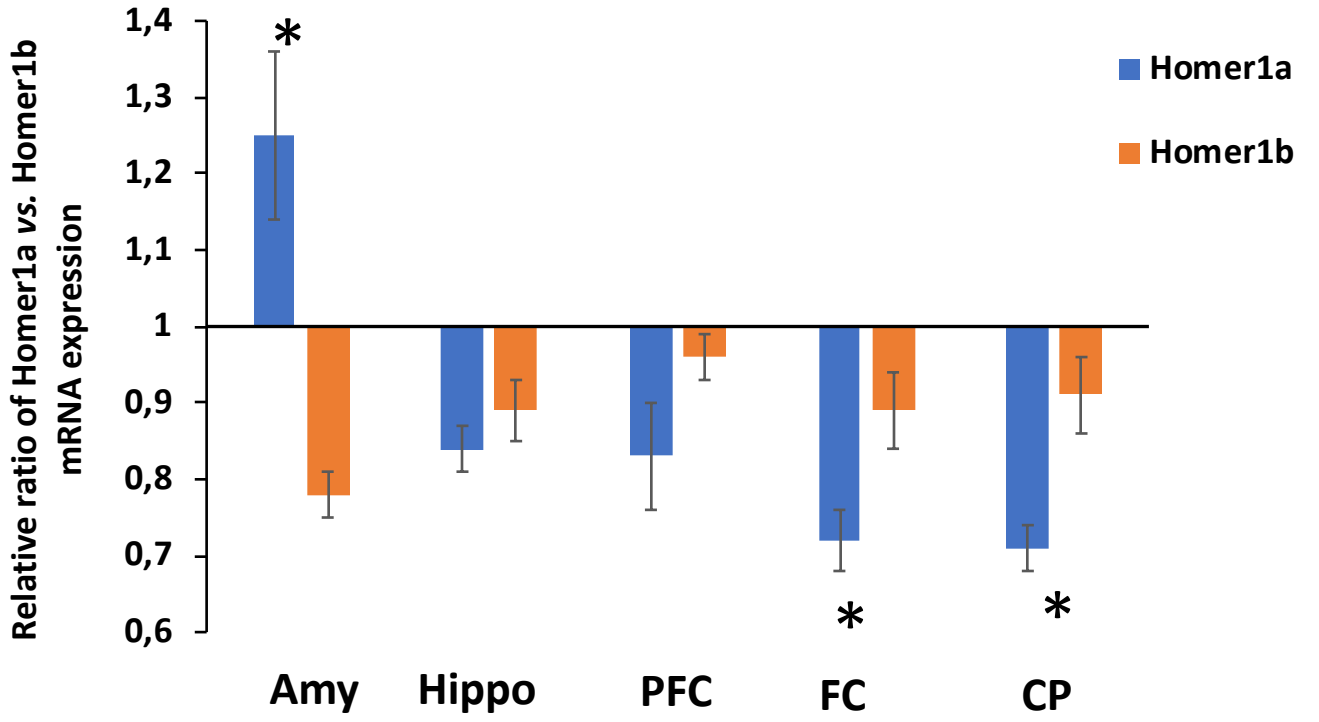
Relative ratio of Homer1a vs. Homer1b mRNA expression
1,4
1,3
1,2
1,1
1
0,9
0,8
0,7
0,6
Homer1a
Homer1b
*
*
*
Amy
Hippo
PFC
FC
CP

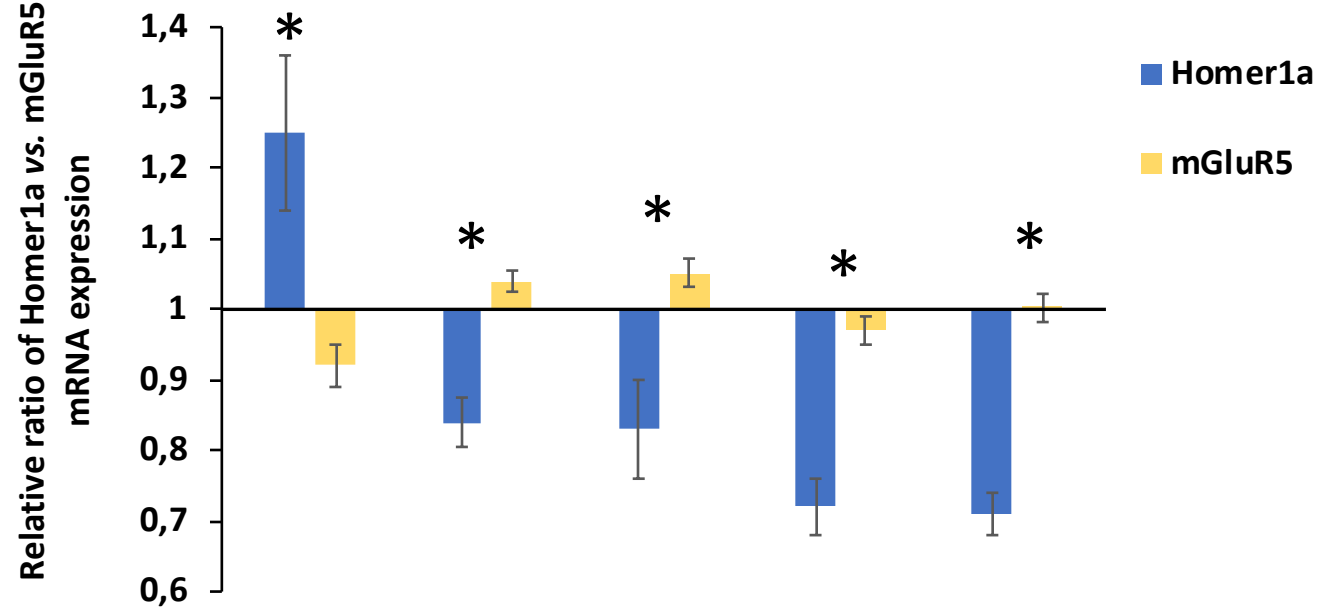
Relative ratio of Homer1a vs. mGluR5 mRNA expression
1,4
1,3
1,2
1,1
1
0,9
0,8
0,7
0,6
Homer1a
mGluR5
*
*
*
*
*

Figure 6

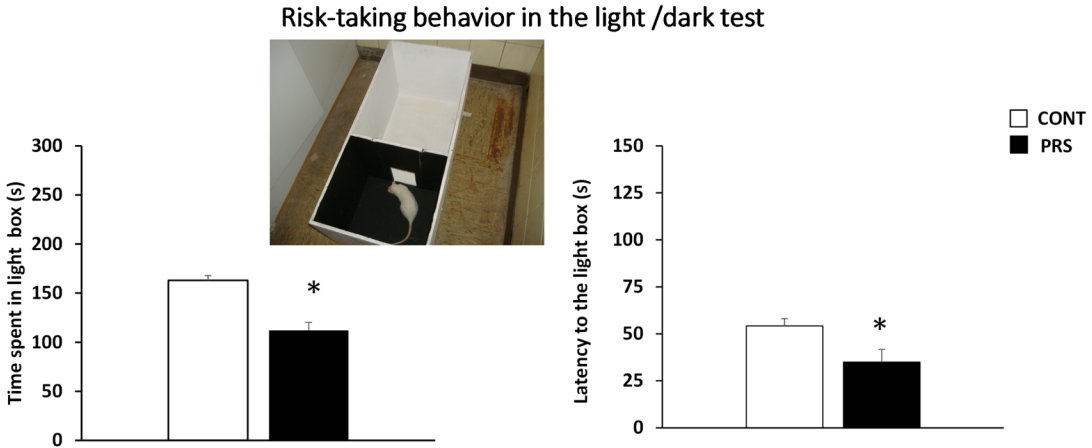
Risk-taking behavior in the light /dark test
Time spent in light box (s)
300
250
200
150
100
50
0
*
Latency to the light box (s)
150
125
100
75
50
25
0
*
CONT
PRS

Figure 7

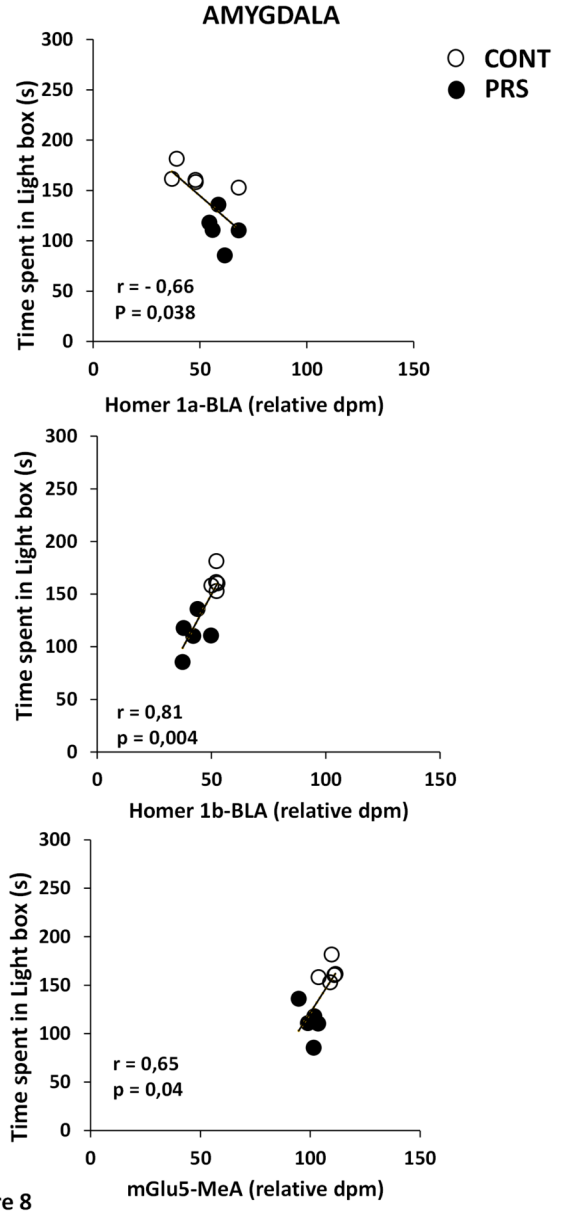
AMYGDALA
CONT
PRS
Time spent in Light box (s)
300
250
200
150
100
50
0
r = - 0,66
P = 0,038
0
50
100
150
Homer 1a-BLA (relative dpm)
Time spent in Light box (s)
r = 0,81
p = 0,004
Homer 1b-BLA (relative dpm)
Time spent in Light box (s)
r = 0,65
p = 0,04
mGlu5-MeA (relative dpm)

Figure 8

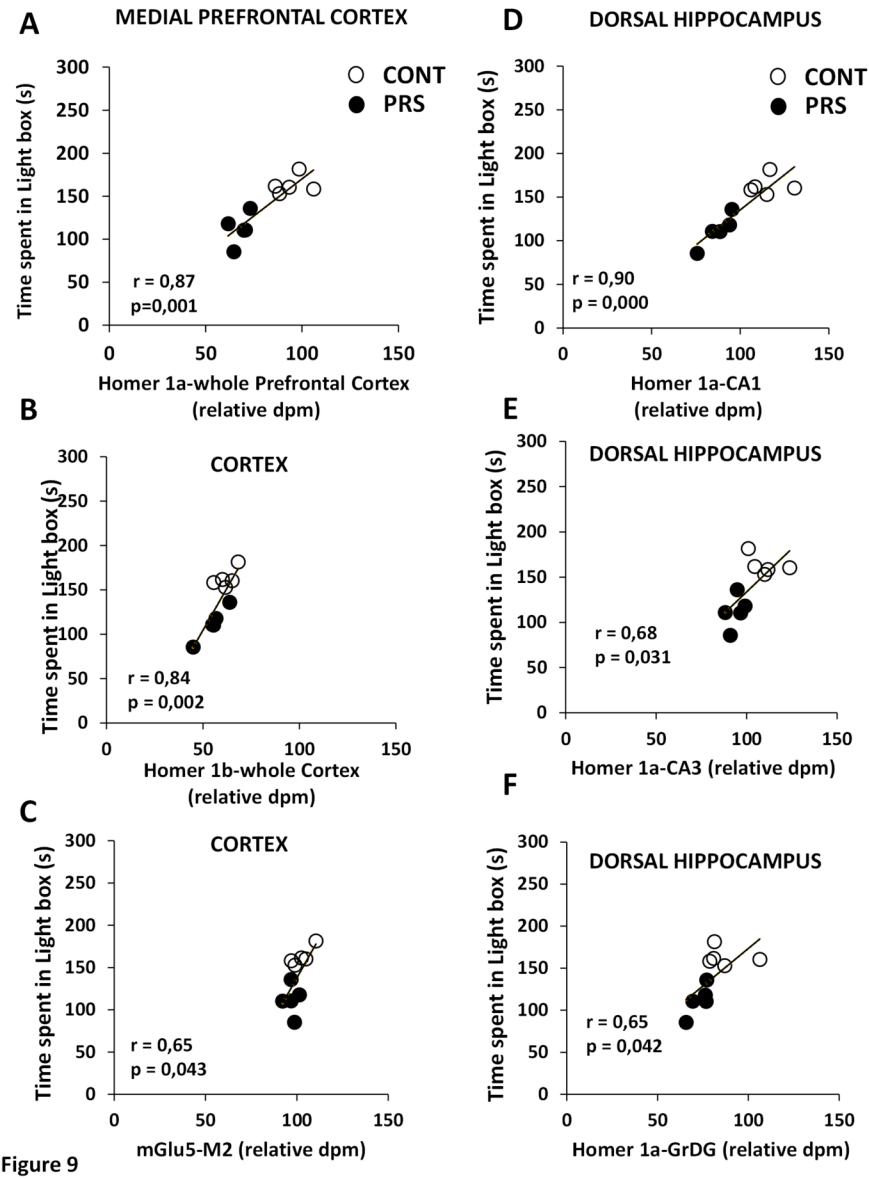
A
MEDIAL PREFRONTAL CORTEX
CONT
PRS
Time spent in Light box (s)
r = 0,87
p=0,001
Homer 1a-whole Prefrontal Cortex (relative dpm)
D
DORSAL HIPPOCAMPUS
CONT
PRS
Time spent in Light box (s)
r = 0,90
p = 0,000
Homer 1a-CA1 (relative dpm)
B
CORTEX
Time spent in Light box (s)
r = 0,84
p = 0,002
Homer 1b-whole Cortex (relative dpm)
E
DORSAL HIPPOCAMPUS
Time spent in Light box (s)
r = 0,68
p = 0,031
Homer 1a-CA3 (relative dpm)
C
CORTEX
Time spent in Light box (s)
r = 0,65
p = 0,043
mGlu5-M2 (relative dpm)
F
DORSAL HIPPOCAMPUS
Time spent in Light box (s)
r = 0,65
p = 0,042
Homer 1a-GrDG (relative dpm)

Figure 9

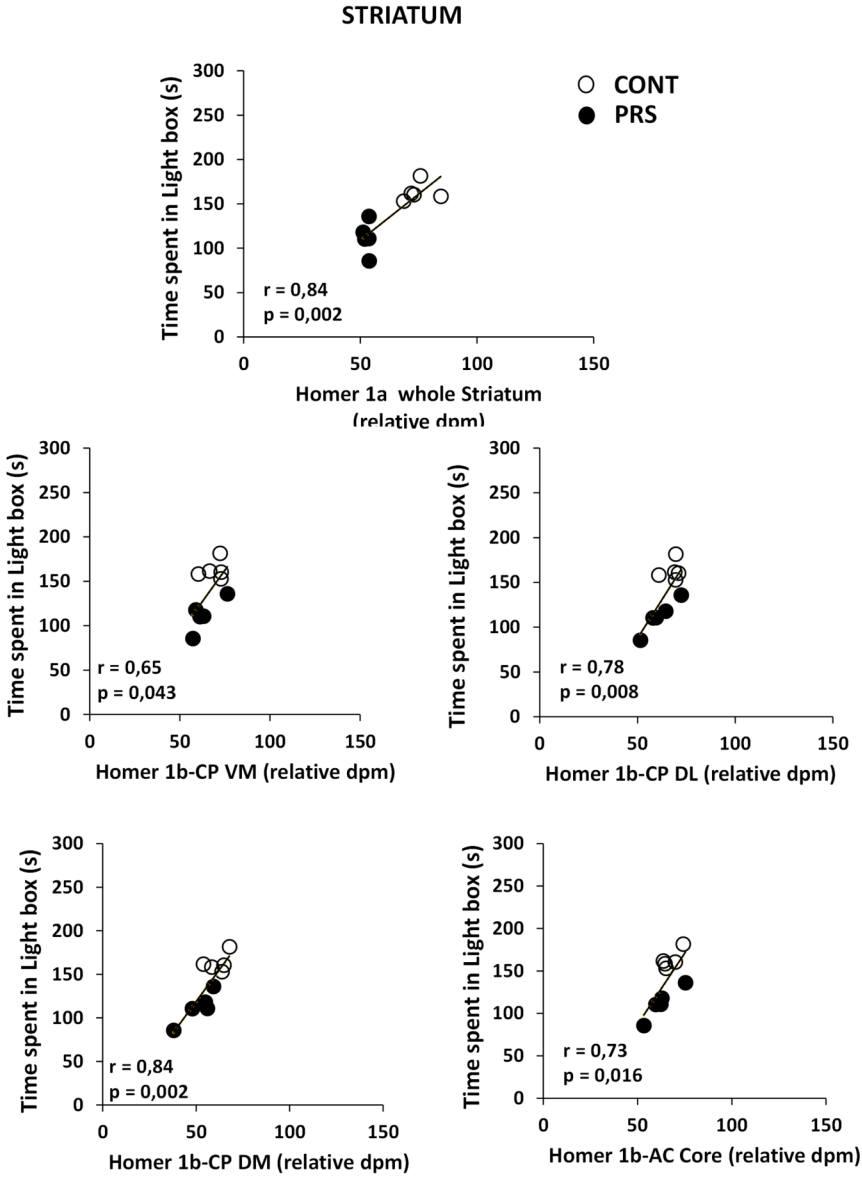
STRIATUM
CONT
PRS
Time spent in Light box (s)
r = 0,84
p = 0,002
Homer 1a whole Striatum (relative dpm)
r = 0,65
p = 0,043
Homer 1b-CP VM (relative dpm)
r = 0,78
p = 0,008
Homer 1b-CP DL (relative dpm)
r = 0,84
p = 0,002
Homer 1b-CP DM (relative dpm)
r = 0,73
p = 0,016
Homer 1b-AC Core (relative dpm)

Figure 10

Probe	cDNA length (bp)	cDNA position	mRNA	Gen-Bank#
Homer1a	48	2527–2574	*Homer1a*	U92079
Homer1b	48	1306–1353	*Homer1b/c*	AF093268
mGluR5	48	3005-3053	*mGluR5*	NM_017012.1

Table 1. Probes for *in situ* hybridization histochemistry.